EXTREME VACUUM TECHNOLOGY INCLUDING CRYOSORPTION, DIFFUSION PUMP AND PRESSURE CALIBRATION STUDIES

QUARTERLY STATUS REPORT NO. 9
1 August - 1 November 1965

Contract NASr-63(06)

MRI Project No. 2675-P

For

Headquarters
National Aeronautics and Space Administration
Attn: Code SC
Washington, D.C. 20546

MRI
MIDWEST RESEARCH INSTITUTE
425 VOLKER BOULEVARD/KANSAS CITY, MISSOURI 64110/AC 816 LO 1-0202

EXTREME VACUUM TECHNOLOGY INCLUDING CRYOSORPTION, DIFFUSION PUMP AND PRESSURE CALIBRATION STUDIES

by

Paul J. Bryant
Charles M. Gosselin

QUARTERLY STATUS REPORT NO. 9
1 August - 1 November 1965

Contract NASr-63(06)

MRI Project No. 2675-P

For

Headquarters
National Aeronautics and Space Administration
Attn: Code SC
Washington, D.C. 20546

MIDWEST RESEARCH INSTITUTE
425 VOLKER BOULEVARD/KANSAS CITY, MISSOURI 64110/AC 816 LO 1-0202

PREFACE

The development of several phases of research relating to vacuum science and technology are included in this program. Mr. George Wise of the NASA Lewis Research Center is the technical monitor. This Quarterly Status Report covers the period from 1 August 1965 to 1 November 1965.

The research activity is conducted in the Physics Department of the Midwest Research Insititute under the direction of Dr. Sheldon L. Levy and Mr. Gordon E. Gross. Research activities were conducted by Dr. Paul Bryant, Mr. Charles Gosselin and Mr. David Moore.

Approved for:

MIDWEST RESEARCH INSTITUTE

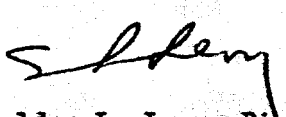

Sheldon L. Levy, Director
Mathematics and Physics Division

6 December 1965

SUMMARY

Experimental measurements as well as a theoretical description of cryosorption are given in this report. Their correlation establishes a solid basis for the prediction of cryopanel operation. The theoretical description includes the development of a new adsorption model and a computer program for the prediction of cryopanel operation with time, pressure, and temperature as variables. This theoretical portion of the program was completed and published during the last quarter as an article in the Journal of Chemical Physics and a reprint is included as Part III of this report.

The experimental portion of the cryosorption work is also described in the present report. Results obtained so far have shown correlation with the theoretical predictions. The onset of second, third, and fourth monolayers of helium occurred near the predicted pressures and within the spacings indicated by the computer program. A condensation effect also was indicated and traced through approximately 19 monolayers. All of the experimental results obtained so far have been for helium adsorbed upon an aluminum cryosurface at 4.28°K.

The experimental results obtained for cryosorption now indicate that the new physical adsorption theory is valid. The results also indicate that the computer program is useful for the prediction of cryopanel operation.

I. INTRODUCTION

The three research phases of this program relate to the development and application of vacuum science and technology. For example, the gas adsorption studies described in this report relate to the design and performance of cryopanels.

The two previous quarterly reports have described results relating to diffusion pump studies and to vacuum gauge calibration work, respectively. Thus, each quarterly report has concentrated on one of the phases of the overall program. The next annual report will summarize the results from each of the three research phases.

II. CRYOSORPTION EXPERIMENTS WITH HELIUM GAS AND ALUMINUM SURFACES

Experimental results have been obtained for comparison with the predicted operation of a cryopanel. Helium gas was allowed to adsorb onto an aluminum surface at 4.28°K. A quartz piezoelectric crystal oscillator is being employed as a microbalance to measure the amount of adsorbed helium. The surface of the quartz crystal is covered with a thin aluminum film which serves as an electrode as well as a cryopanel material. The adsorbed helium atoms add to the mass of the crystal and causes a damping of the oscillations; thus, the resonant frequency of the system is a function of the amount of adsorbed helium.

The electronic oscillator circuit which was constructed specifically for this microbalance application is capable of maintaining the crystal at 5 Mc. with mean variation of 0.1 cycle. The counter and digital-to-analog converter circuit used for data recordings are capable of transmitting this high accuracy to a chart recorder in 10 sec. data bits. For rapid data collection the time interval for data summation is reduced to 1 sec. and the frequency count is accurate to 1 cycle. The data for helium adsorption indicate a sensitivity of 200 cycles/monolayer. That is, with rapid data collection and 1 sec. recording times the microbalance can measure 1/200 of a helium monolayer.

Data for helium adsorption have been recorded in several different ways. The amount of helium in the gas phase versus the adsorbed phase was recorded for pressures from 10^{-11} torr to 10^{-3} torr and for adsorbed quantities from a fraction of a monolayer to 19 monolayers while pure helium was being admitted to the system. However, for low pressures this dynamic process did

not permit equilibrium pressure data to be collected in a reasonable time period. Therefore, individual pressure measurements were obtained under equilibrium conditions for specific surface coverages. Another method of data collection was based on a uniform time rate of helium gas admission to the system. The fraction of helium pumped by the microbalance cryosurface was then recorded versus time with the remaining fraction allotted to the gas phase.

The summation of data for helium pumped by an aluminum cryosurface at 4.28°K shows the following features: a pressure below the recording limit of standard UHV gauges (both an ion gauge and a cold cathode gauge were employed) for fractional monolayer coverage; a pressure of 10^{-5} torr for initiation of second monolayer coverage; third and fourth monolayer coverages in the 10^{-4} torr range; and a rapid build-up of adsorbed layers with pressure rise around 10^{-3} torr. Each of these experimental observations shows general agreement with the operation of a liquid helium temperature cryopanel as predicted by the theoretical phase of this program. The theoretical development and predictions are presented in Part III of this report.

III. PHYSICAL-ADSORPTION ISOTHERM BASED ON A TRIANGULAR-SITE MODEL

(The research work covered by this section of the report was submitted for publication to The Journal of Chemical Physics. The reprint from this Journal is included as part of this report.)

Reprinted from THE JOURNAL OF CHEMICAL PHYSICS, Vol. 43, No. 4, 1184–1189, 15 August 1965
Printed in U. S. A.

Physical-Adsorption Isotherm Based on a Triangular-Site Model*

LYLE H. TAYLOR, WILLIAM W. LONGLEY, JR., AND PAUL J. BRYANT
Midwest Research Institute, Kansas City, Missouri

(Received 10 February 1965)

A multilayer physical-adsorption-isotherm theory is developed; it assumes that a gas atom cannot be physically adsorbed in an upper layer unless there is a triangular array of three adsorbed atoms in the layer below forming a site for adsorption. Neighbor interactions via Lennard-Jones intermolecular potentials are included in the calculation of the adsorption energy. The resultant isotherm is linear for low coverages, indicates a horizontal interaction correction to the Langmuir adsorption isotherm when there is only first-layer coverage, and may yield a series of steps for sufficiently low temperature. Numerical adsorption isotherms for He on glass at 4.28° and 77°K are presented. The former isotherm exhibits distinctive steps when each layer is condensed, whereas the latter isotherm is quite smooth.

I. INTRODUCTION

MANY theories of physical adsorption have been proposed, and many modifications of these theories have been developed. This intensive effort is understandable since the phenomenon is extremely interesting and would seem to lend itself to precise experimental measurements and accurate theoretical descriptions. Experience has shown that physical adsorption is a function of many variables, e.g., molecular interactions, surface roughness, adsorption-site models, molecular vibrational states, etc. To avoid excessive cumbersomeness and difficulty, it is customary for any theory to incorporate only a few variables and to approximate or to ignore the remainder. This paper is no exception in that regard.

The derivation presented here has some different assumptions, but is analogous to the derivation, via the discipline of statistical mechanics, of the Brunauer–Emmett–Teller (BET) adsorption isotherm.[1,2] There are also similarities to Halsey's triangular-site model.[3,4] In the new theory, the mathematically flat surface with S_1 fixed sites is borrowed from the BET theory. The variation of site energy with coverage of all permitted layers is considered in greater detail than in either of the above-mentioned theories. This energy treatment is based on a Bragg–Williams model[5] for occupation assignment.

Section II details the numerous approximations used in this paper and describes the statistical-mechanical theory used to derive the physical-adsorption-isotherm equations based on a triangular-site model. Since treating molecular interactions causes the adsorption energy to vary as a function of coverage in all layers, an "effective" adsorption energy is defined in Sec. III. The adsorption isotherm equations are discussed in Sec. IV, and an iteration technique is presented. Two specific isotherms for helium on glass are calculated from this theory and discussed in Sec. V.

II. GENERAL THEORY

The mathematically flat surface of the BET theory is used; however, the single-particle–single-site model of the BET theory is replaced by the more aesthetic triangular-site model of Halsey,[4] i.e., it is assumed that a particle cannot be adsorbed in an upper layer unless there is a triangular array of three adsorbed particles forming a site for adsorption. The BET and triangular-site models are compared diagrammatically in Fig. 1.

Let X_j represent the number of adsorbed particles in the jth layer. Then the total number of adsorbed

* This work was supported by the National Aeronautics and Space Administration, Headquarters, Washington, D. C., under Contract NASr–63(06).

[1] W. C. Band, *Introduction to Quantum Statistics* (D. Van Nostrand Company, Inc., New York, 1955).

[2] S. Brunauer, P. H. Emmett, and E. Teller, J. Am. Chem. Soc. **60**, 309 (1938).

[3] G. D. Halsey, Advan. Catalysis **4**, 259 (1952).

[4] G. Halsey, J. Chem. Phys. **16**, 931 (1948).

[5] T. L. Hill, *Introduction to Statistical Thermodynamics* (Addison-Wesley Publishing Company, Inc., Cambridge, Massachusetts, 1960).

particles A is given by

$$A=\sum_{j=1}^{J}X_j,$$

where J is the total number of layers containing adsorbed particles. In addition, let each layer be mathematically flat and contain S_1 fixed sites in the same configuration as those of the first layer but laterally displaced for close packing. Furthermore, assume that the probability of a given fixed site being occupied is θ_j, where $\theta_j=X_j/S_1$ is the fractional occupancy of the jth layer. This choice of occupation probability is consistent with the gas particles striking the adsorbing sites at random and being unable to migrate over the surface.

The next problem is to find the number of sites available for an adsorbed particle in the jth layer. The triangular-site model and the close-packed-array assumption make this quantity equal to the total number of possible sites, neglecting the site occupation rule, times the probability of simultaneous occupation of three adjacent fixed sites in the preceding layer, i.e.,

$$S_j=X_{j-1}\theta_{j-1}^2,\ X_0=S_1,\ \theta_0=1. \qquad (1)$$

Equation (1) replaces $S_j=X_{j-1}$ in the BET theory. Now S_j need not be an integer. The generalized factorial, the gamma function, is used in the calculation of the total number W of independent ways to assign N indistinguishable particles to the over-all adsorption system (gas and adsorbate surface):

$$W=\prod_{j=1}^{\infty}\left(\frac{\omega_j^{n_j}}{n_j}\right)\frac{\Gamma(S_j+1)}{\Gamma(X_j+1)\Gamma(S_j-X_j+1)}, \qquad (2)$$

where ω_i is the degeneracy weight of the ith energy level ϵ_i of the gas and n_i is the number of gas particles in that energy level.

The statistical problem is to find the numbers X_j and n_j that give a maximum value to $\sigma_s=\ln W$, under the restrictions of a given total number of particles N and a given total energy E. The constraints on the system are given by

$$N=\sum_{j=1}^{\infty}(n_j+X_j), \qquad E=\sum_{j=1}^{\infty}(n_j\epsilon_j-X_jW_j), \qquad (3)$$

where W_j is the average energy of adsorption for each adsorbed particle in the jth layer.

Since N and E are constant and σ_s is a maximum, their variations must vanish. In performing the variational calculation, it is convenient to define the "effective" adsorption energy E_j, which obviously depends on the molecular interactions and interlayer-adsorption-energy variations, as follows:

$$E_j=W_j+\sum_{i=1}^{J}\theta_i\frac{dW_i}{d\theta_j}. \qquad (4)$$

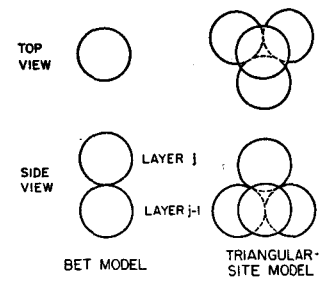

FIG. 1. Site models.

The variational calculation yields the following equations:

$$d\sigma_g/dn_i=\alpha+\beta\epsilon_i, \qquad (5)$$

$$d\sigma_a/dX_j=\alpha-\beta E_j, \qquad (6)$$

where $\sigma_s=\sigma_g\sigma_a$, σ_a being that part of the product pertaining only to the adsorbed particles and σ_g that part pertaining only to the gas particles.

Equation (5) is the classical equation of an ideal gas of Boltzmann particles treated separately from the adsorbed layers. Assuming n_i to be very large leads to the identification of α and β in terms of the chemical potential μ and the absolute temperature T of the gas phase[1]:

$$\alpha=-\mu/k_0T, \qquad \beta=1/k_0T, \qquad (7)$$

where k_0 is Boltzmann's constant. The ideal gas law also follows:

$$\begin{aligned} &pV=N_gk_0T,\\ &N_g=k_0^{-1}KV(MT)^{\frac{3}{2}}\exp(\mu/k_0T),\\ &K=(2\pi k_0)^{\frac{3}{2}}k_0h^{-3}, \end{aligned} \qquad (8)$$

where V is the volume, p is the pressure, M is the mass of a gas particle, and h is Planck's constant. These results are derived from Boltzmann statistics which are valid[1] when α exceeds 3.

It is now convenient to define a new parameter γ_j, such that

$$\gamma_j=\exp[-(\mu+E_j)/k_0T] \qquad (9)$$

and to evaluate this new parameter in terms of physically measurable parameters. From Eqs. (8) and (9) one obtains

$$\gamma_j=(KM^{\frac{3}{2}}T^{\frac{5}{2}}/p)\exp(-E_j/k_0T). \qquad (10)$$

Equation (6) can now be written as

$$d\sigma_a/d\theta_j=S_1\ln\gamma_j. \qquad (11)$$

The latter expression is the basic equation to solve in deriving the adsorption isotherm. By using Stirling's approximation for large arguments of the gamma functions in Eq. (2) and by differentiating the result, the

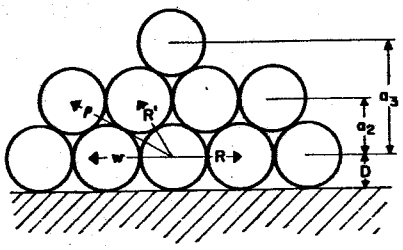

FIG. 2. Adsorption geometry.

left-hand side of Eq. (11) is evaluated. The final result is

$$\gamma_j=[(\theta_{j-1}{}^2-\theta_j)/\theta_j][\theta_j{}^2/(\theta_j{}^2-\theta_{j+1})]^{\frac{1}{2}}i^2. \quad (12)$$

The triangular-site physical-adsorption isotherm is obtained from the simultaneous solution of Eqs. (10) and (12).

III. EFFECTIVE ADSORPTION ENERGIES

The energy of adsorption W_j is defined as the difference between the energy of a free particle at rest and the average energy of an adsorbed particle in the jth layer. Equation (4) shows that the effective adsorption energy E_j is completely determined when all the W_j's are known.

It is assumed that the intermolecular potential ϕ between two adsorbed molecules can be closely approximated by the Lennard-Jones $(n-m)$ potential for spherically symmetric molecules:

$$\phi(r)=\frac{\epsilon}{m-n}\left(\frac{m^m}{n^n}\right)^{1/(m-n)}\left[\left(\frac{\sigma}{r}\right)^m-\left(\frac{\sigma}{r}\right)^n\right], \quad m>n, \quad (13)$$

where r is the distance between the molecules, σ is the distance of closest approach of two molecules which collide with zero initial relative kinetic energy, and ϵ is the maximum energy of attraction of the two molecules when the repulsive term is also considered.[6] If R represents the equilibrium distance between the adsorbed molecules, it is necessary that ϕ be a minimum at R, i.e.,

$$R=(m/n)^{1/(m-n)}\sigma. \quad (14)$$

Since ϕ is an energy per pair of gas molecules, and since W_j is an energy per gas molecule, each pair that includes one specific molecule will contribute $\frac{1}{2}\phi(r)$ to W_j for that molecule.

The intermolecular potential ϕ_s between an adsorbed molecule and an adsorbent molecule is approximated by another Lennard-Jones potential:

$$\phi_s(r)=\frac{\epsilon_s}{k-l}\left(\frac{k^k}{l^l}\right)^{1/(k-l)}\left[\left(\frac{\sigma_s}{r}\right)^k-\left(\frac{\sigma_s}{r}\right)^l\right], \quad k>l. \quad (15)$$

Since the change of potential at an adsorbent molecule is not considered, the entire value of ϕ_s will be assigned to W_j for the adsorbed molecule.

The term "physical adsorption" can now be explicitly defined as that adsorption for which $k>l>3$ and $m>n>3$. In other words, attractive forces arising from ionic charges and permanent dipoles are excluded from consideration.

Integration of the intermolecular potential of gas and adsorbent molecules over the volume occupied by the solid leads to an evaluation of the adsorbent contribution W_{sj} to the adsorption energy W_j. The integration implies that the intermolecular potentials are additive. This latter assumption is probably more serious than any made thus far,[7] but it is necessary for any simple and usable theory.

With the surface located a distance D below the centers of the adsorbed molecules in the first layer (see Fig. 2), W_{s1} is given by

$$W_{s1}=W_s$$
$$=2\pi\epsilon_s N_0 D^3\left(\frac{k}{l-2}\right)^{k/(k-l)}\left(\frac{k-2}{l}\right)^{l/(k-l)}\frac{1}{(k-3)(l-3)}, \quad (16)$$

where

$$D=[(l-2)/(k-2)]^{1/(k-l)}\sigma_s \quad (17)$$

and N_0 is the number of adsorbent molecules per unit volume. The energy of interaction W_{s1} was chosen to be a maximum for the particular potential used, thus explaining why D is less than σ_s.

The adsorbate layers are assumed to be equally spaced at intervals a from each other. Thus, the distance between the first layer and the jth layer (as indicated in Fig. 2) is a_j, where

$$a_j=(j-1)a=Dd_j. \quad (18)$$

The adsorbent contribution to W_j is given by

$$W_{sj}=\frac{W_s}{k-l}\left[\frac{k-3}{(1+d_j)^{l-3}}-\frac{l-3}{(1+d_j)^{k-3}}\right]. \quad (19)$$

An adsorbed molecule interacts with the adsorbent and all other adsorbed molecules. The interactions between the molecules of the ith layer and a specific molecule in the jth layer are labeled W_{ij}. The adsorption energy can be determined by summing W_{sj}, which has already been evaluated, and all W_{ij}. The W_{ij} are individually evaluated below by treating the nearest-neighbor interactions exactly and approximating the remaining interactions.

The evaluation of $W_{j+2,j}$ is interesting since the molecules in the $(j+2)$th layer may be positioned in two possible ways. If these molecules lie above those in the jth layer, the hexagonal close-packed crystalline structure results. Otherwise, the face-centered-cubic structure is obtained. But there is virtually no differ-

[6] J. O. Hirschfelder, C. F. Curtiss, and R. B. Bird, *Molecular Theory of Gases and Liquids* (John Wiley & Sons, Inc., New York, 1954).

[7] J. R. Sams, G. Constabaris, and G. D. Halsey, Jr., J. Chem. Phys. **36**, 1334 (1962).

ence in energies between these two crystalline structures. Therefore, the interaction energy is evaluated by representing the $(j+2)$th layer as a plane and integrating over it. The result is

$$W_{lj}=\theta_l z(|a_l-a_j|), \tag{20}$$

where

$$z(r)=\frac{2\pi\epsilon r^2}{\sqrt{3}(m-n)R^2}\left(\frac{m^m}{n^n}\right)^{1/(m-n)}\left[\frac{1}{n-2}\left(\frac{\sigma}{r}\right)^n-\frac{1}{m-2}\left(\frac{\sigma}{r}\right)^m\right]. \tag{21}$$

The subscript l is used in Eq. (20) since it can be used for any layer that does not contain a nearest neighbor to the particle in the jth layer. Equation (20) will be used for all l except $j-1$, j, and $j+1$.

The evaluation of the $W_{j-1,j}$ interaction energy is straightforward and is done by summing over the three nearest neighbors at distance R' (see Fig. 2) and by integrating over the remainder of the $(j-1)$th layer. The result is

$$W_{j-1,j}=[\theta_{j-1}z(\rho)-\tfrac{3}{2}\phi(R')]f_j', \tag{22}$$

where $f_j'=1-\delta_j^1$ relates f_j' to the Kronecker delta and ρ is, for the moment, an arbitrary distance used in both the $(j-1)$th and $(j+1)$th layers as illustrated in Fig. 2.

The $W_{j-1,j}$ interaction energy is treated in a like manner. The integrated term is exactly analogous to that in Eq. (22), but the factor 3/2 appearing in the other term must be replaced by a probability function, because the three nearest neighbors are no longer involved in forming the triangular adsorption site and, hence, cannot be assured of existence. This probability function P_j is evaluated as

$$P_j=(\theta_{j+1}/3\theta_j^3)P_{j-1}^2, \qquad P_0=3\theta_1. \tag{23}$$

Therefore, the contribution of the $(j+1)$th layer to W_j is

$$W_{j+1,j}=\theta_{j+1}z(\rho)-\tfrac{1}{2}P_j\phi(R'). \tag{24}$$

Likewise, the W_{jj} interaction energy is evaluated to be

$$W_{jj}=\theta_j z(w)+P_{j-1}\epsilon, \tag{25}$$

where w is another arbitrary distance (see Fig. 2).

The values of w and ρ must be ascertained in a systematic manner. The chosen method of determining w is to require the integration result (for $\theta_j=1$) at w to equal the correct result obtained by actually summing over the six next-nearest neighbors lying within the jth layer. Thus, w is determined to be

$$w=[2\pi/(n-2)\sqrt{3}]^{1/(n-2)}\sqrt{3}R. \tag{26}$$

Using a comparable argument for ρ, we obtain

$$\rho=[4\pi(4R^2+3a^2)/\sqrt{39}(n-2)R^2]^{1/(n-2)}(\tfrac{4}{3}R^2+a^2)^{\frac{1}{2}}. \tag{27}$$

The adsorption energy is determined by adding the above interaction energies to give

$$W_j=W_{sj}-\tfrac{1}{2}(3f_j'+P_j)\phi(R')+P_{j-1}\epsilon+\theta_j z(w)+(f_j'\theta_{j-1}+\theta_{j+1})z(\rho)+\sum_{i=1}^{j-2}\theta_i z(a_j-a_i)+\sum_{i=j+2}^{J}\theta_i z(a_i-a_j). \tag{28}$$

Equation (4) can now be applied to this equation to yield the effective adsorption energy

$$E_j=W_{sj}+2P_{j-1}\epsilon-\tfrac{1}{2}(3+P_{j-1}\theta_{j-1}/\theta_j)f_j'\phi(R')-\sum_{i=j+1}^{J}\frac{2^{i-j-1}\theta_i[P_{i-1}\epsilon-P_i\phi(R')]}{\theta_j}+2\theta_j z(w)+2(f_j'\theta_{j-1}+\theta_{j+1})z(\rho)+2\sum_{i=1}^{j-2}\theta_i z(a_j-a_i)+2\sum_{i=j+2}^{J}\theta_i z(a_i-a_j). \tag{29}$$

IV. ADSORPTION ISOTHERM

The triangular-site physical-adsorption equations cannot be solved exactly but must be solved iteratively. The kth iterative solution is obtained by rearranging Eq. (12) to give

$$\theta_j^{(k)}=\theta_{j-1}^3[1+\gamma_j(1-\theta_{j+1}\theta_j^{-3})^{3\theta_j^2}]^{-1}, \tag{30}$$

where the right-hand side is evaluated by using the kth iterative values for all θ_i, $i<j$ and the $(k-1)$th iteration values for all θ_i, $i\geq j$. The exact theory is obtained when the iteration converges.

Starting values for the exact theory can be obtained either from intelligent guesses or from the approximate theory. The approximate theory, which sets $\theta_i=0$ for $i>j$ and neglects the θ_j dependence of γ_j, has many interesting properties. For example, when

$$p\ll KM^{\frac{1}{2}}T^{\frac{1}{4}}\exp(-W_s/k_0T),$$
$$\theta_1\approx(p/KM^{\frac{1}{2}}T^{\frac{1}{4}})\exp(W_s/k_0T), \tag{31}$$

it is shown that the percent coverage is directly proportional to the pressure. This linear dependence has been verified for Kr, Ar, and Ne on P33 carbon black.[8] In the range where Eq. (31) is invalid but only monomolecular adsorption is occurring, the approximate theory reduces to the conventional Langmuir adsorption isotherm for a single adsorbed layer.

The exact theory is based on a solid-state approach to the adsorbed layers and must become invalid when the temperature is above the melting point of the adbate or if the resultant crystalline structure is neither face-centered cubic nor hexagonal close packed. (Evidence[9] has been presented suggesting that helium

[8] G. Constabaris, J. H. Singleton, and G. D. Halsey, Jr., J. Phys. Chem. **63**, 1350 (1959).

[9] J. G. Aston, S. V. R. Mastrangelo, and R. J. Tykodi, J. Chem. Phys. **23**, 1633 (1955).

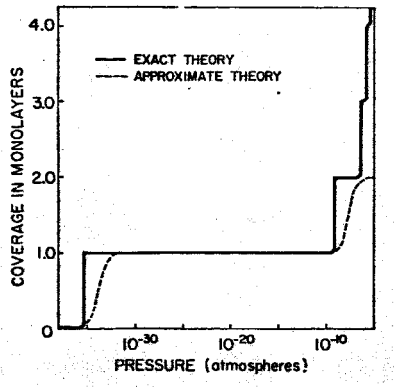

FIG. 3. Adsorption isotherm for helium on porous glass at 4.28°K.

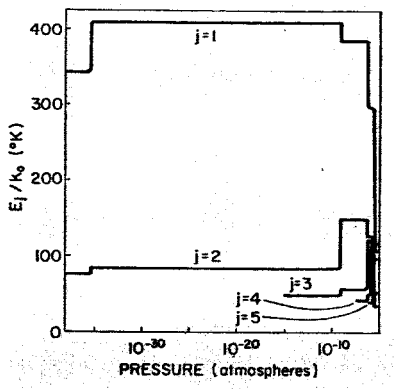

FIG. 5. Effective adsorption energy for helium on porous glass at 4.28°K.

adsorbs onto titanium dioxide in a solid-state lattice.) One of the more interesting features of the exact theory is that E_j passes through a maximum and then decreases as the pressure is increased. However, a close examination of Eq. (29) shows that this maximum should *almost* coincide with the event of $\theta_{j+1}=\theta_j^2$, and from Eq. (30) this equality cancels any variation of γ_j. Thus far, numerical calculations (see Sec. V) have shown the cancellations to be the case.

V. NUMERICAL RESULTS

In order to make numerical predictions, certain parameters needed to evaluate the E_j's are based on measurements by different methods. Halsey,[10] by fitting adsorption data to a 3-∞ potential, has measured the values of D and W_s for six different adsorbates on porous glass and eight adsorbates on P33 graphitized carbon black. Gas–gas force constants, σ and ϵ, are given in Hirschfelder, Curtiss, and Bird.[6] Based on the assumption of ideal hexagonal close-packed or face-centered cubic structure ($R'=R$), the values of a, w, and ρ can be calculated from the gas–gas R value.

The approximate and exact theories were both applied to calculate triangular-site adsorption isotherms for helium on porous glass at temperatures of 4.28° and 77°K. The former isotherm is plotted in Fig. 3 where "monolayer coverage" θ is defined as the ratio of the total number of adsorbed molecules to the number of sites present on the adsorbent, i.e., A/S_1. The approximate theory appears to be fairly good for $\theta<2$, but fails badly at higher coverages. However, the most striking features of Fig. 3 are the very abrupt steps exhibited by the exact theory. This apparent condensation is physically attributable to the intralayer molecular interactions. If the classical second virial coefficient value[6] of ϵ/k_0, 6.03°K, were used, the pressures which permit second- and higher-level coverages to become appreciable would be raised by a factor of ~100. Thus, the theory indicates a strong dependence on the value of ϵ.

The adsorption energies and effective adsorption energies are plotted in Figs. 4 and 5, respectively. Note that the adsorption energies are monotonically increasing, whereas the effective adsorption energies for the first three layers exhibit maxima. However, no physical effect of the maxima is predicted since, whenever E_j decreases, the multiplicative factor of γ_j in Eq. (30) is always zero due to filling of the $(j+1)$th layer.

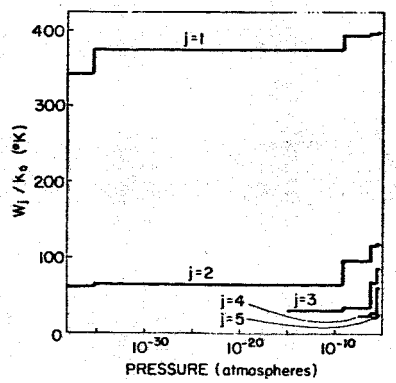

FIG. 4. Energies of adsorption for helium on porous glass at 4.28°K.

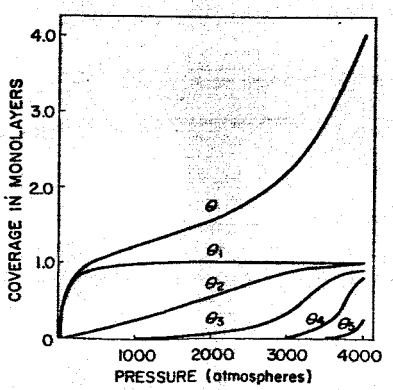

FIG. 6. Adsorption isotherm for helium on porous glass at 77°K.

[10] G. D. Halsey, Jr., Trans. Natl. Vac. Symp. **1961**, 119 (1962).

The triangular-site adsorption isotherm for helium on glass at 77°K is plotted in Fig. 6. Notice the smooth curves and partially filled layers as contrasted with the single-layer condensation steps of Fig. 3. As expected, the adsorption energies shown in Fig. 7 are smoothly and monotonically increasing. Contrary to the results at 4.28°K, the effective adsorption energies plotted in Fig. 8 exhibit maxima which do not coincide exactly with the vanishing of the γ_j multiplier in Eq. (30). The physical effect of this noncoincidence is shown in Fig. 6 by the gradual approach of θ_1 and θ_2 to 1. Another interesting result, excluding the first two layers, is indicated in Fig. 8 by the extremely high effective adsorption energy for the top layer at very low coverages.

VI. CONCLUSIONS

The *numerical* isotherms given in the previous section cannot be interpreted as bona fide predictions, e.g., in Fig. 3 the saturation pressure of helium is around 10^{-5} atm, whereas the actual saturation pressure is, of course, 1 atm. The error caused by not using weakly degenerate quantum statistics for the gas affects the higher-pressure data of Fig. 6 to some extent. The improper saturation pressure is probably related to the use of the Bragg–Williams model. But more sophisticated models[11] also have inherent difficulties. However,

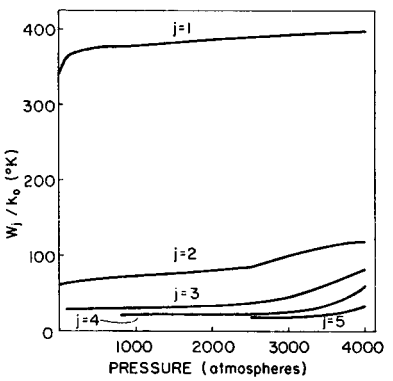

FIG. 7. Energies of adsorption for helium on porous glass at 77°K.

[11] P. C. Hemmer, J. Math. Phys. **5**, 75 (1964).

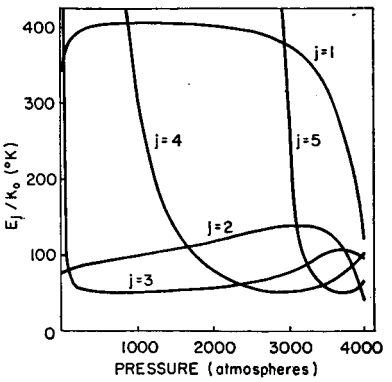

FIG. 8. Effective adsorption energy for helium on porous glass at 77°K.

the numerical isotherms are good examples of adsorption isotherms which may be obtained from the theory. For example, single-layer condensation steps similar to those in Fig. 3 have been observed for krypton on P33 carbon black by Singleton and Halsey,[12] who attribute them to the flatness of the surface—a basic assumption of this paper. On the other hand, the higher-temperature adsorption isotherm of Fig. 6 has the general appearance of many published isotherms.

The main difficulty in using the triangular-site adsorption isotherm is in obtaining values of D, W_s, a, σ, and ϵ. However, Halsey[10] has measured D and W_s for two adsorbents and 11 adsorbates. The interlayer spacing a is not accurately known. The well-published gas–gas values of σ and ϵ can be used, although Steele[13] found that for helium R increased 30% when the helium was adsorbed. Moreover, for argon on P33 carbon black, Sams *et al.*,[7] observed that the Lennard-Jones (6–12) force constants were changed by about 20% from the gas–gas values. A combination of the proper set of W_s, ϵ, R, and a values may reduce the present need for a saturation-pressure correction. Indeed, the theory does suggest that data for the difficult systems of helium and any solid at very low temperatures might be fitted by proper choice of parameters.

[12] J. H. Singleton and G. D. Halsey, Jr., Can. J. Chem. **33**, 184 (1955).

[13] W. Steele, Jr., J. Chem. Phys. **25**, 819 (1956).